Available online at www.sciencedirect.com

ScienceDirect

www.elsevier.com/locate/jes

JES JOURNAL OF ENVIRONMENTAL SCIENCES

www.jesc.ac.cn

Antibiotic contamination control mediated by manganese oxidizing bacteria in a lab-scale biofilter

Yanan Cai, Jing He, Jinkang Zhang, Jicheng Li*

School of Environmental and Municipal Engineering, Qingdao University of Technology, Qingdao 266033, China

ARTICLE INFO

Article history:
Received 30 March 2020
Revised 21 May 2020
Accepted 21 May 2020
Available online 12 June 2020

Keywords:
Antibiotics Biofilter
Manganese oxidizing bacteria
Manganese oxide
Metagenomic sequencing

ABSTRACT

Antibiotic micro-pollution is usually found at the ng/L–level in drinking water sources or discharge water of wastewater treatment plants. In this study, a novel approach mediated by manganese oxidizing bacteria (MnOB) in a biofilter was developed to control the pollution. The results indicated that the biogenic manganese oxide (MnO_x) produced during the oxidation of the feeding manganese ions could coat the surface of the filtering sand effecting the simultaneous removal of antibiotics. It was found that the removal of antibiotics is insured as long as the feeding manganese was well removed and was not influenced by the hydraulic loading. The growth rate of the MnOB group revealed that the antibiotic concentration at 50 and 100 ng/L promoted their activity, but it was inhibited at 500 and 1000 ng/L. The structure of the bacterial community was stable in the presence of antibiotics (50 ng/L), but their extracellular processes changed. The removal performance of the feeding manganese seemed to relate to the extracellular processes of the dominant bacterial genus. Moreover, the freshly formed MnO_x was a buserite-like material that was rich in Mn(III) and Mn(IV) (94.1%), favoring the degradation. The biofilter did not generate additional antibiotic resistant genes in the presence of antibiotics.

Introduction

In recent years, the abuse of pharmaceuticals and personal care products has attracted attention (Bu et al., 2016). Antibiotics are produced and used in large quantities around the world (Zhang et al., 2015). They are frequently detected at the ng/L–level in drinking water resources and discharge water of wastewater treatment plants. Therefore, antibiotics are potential threats to living organisms and humans and their presence must be controlled in the environment (Ferri et al., 2017).

The element manganese is abundantly available on the Earth. The mechanism of electronic transfer between Mn(IV)/Mn(III) and Mn(II) cause the manganese cycle on earth. In addition to the catalytic properties of manganese oxides (Wang et al., 2019, 2020), organic substances can also provide electrons for the conversion of Mn, that is, the Mn(IV)/Mn(III) contained in manganese oxides can also oxidize organic matters. Therefore, synthetic or natural manganese oxides are cost-effective and widely used to control organic contamination. They are also applied to degrade antibiotics. Li et al. (2017) demonstrated that the oxidation of thioether and olefin, hydrolysis, and decarboxylation were the main transformation pathways during the degradation of cefazolin by δ-MnO_2. Pal et al. (2017) found that a synthesized MnO_2 nanosheet could degrade the tetracycline group of antibiotics. Liu et al. (2009) reported that sulfadiazine could be degraded and even mineralized by two birnessites, two pyrolusites, three cryptomelanes, and one ramsdellite. These experiments were conducted with antibiotics at the mg/L level, while the efficiency in removing the trace antibiotics (ng/L) was still unclear.

* Corresponding author.
E-mail: cya_yanan@163.com (Y. Cai).

https://doi.org/10.1016/j.jes.2020.05.024

In the biogeochemical cycles of the Earth, manganese-oxidizing bacteria (MnOB) usually act as a driver in the conversion of Mn(II) to Mn(IV)/Mn(III), producing manganese oxides. Similar to those synthetic or matured oxides, the freshly-formed biogenic manganese oxide (MnO_x) can degrade organic matters. Moreover, MnO_x has a relatively poor crystallinity. Remucal and Ginder-Vogel (2014) conclude that the poor crystallinity of MnO_x can increase the activity in the degradation process. Because MnO_x is *in situ* generated, MnOB can be used as a mediator to degrade antibiotics. Previous studies have revealed that MnOB can mediate the degradation of organic matters, e.g., antibiotics (Tu et al., 2014), 17α-ethinylestradiol (Sabirova et al., 2008), and bisphenol A and nonylphenol (Zhang et al., 2019). However, these studies show that MnOB is usually purely cultivated in a medium. It should be noted that the oxidation of manganese is a prerequisite for the degradation, but the manganese ion, as the necessary matrix of MnOB, is also a water quality indicator. The degradation mediated by MnOB is similar to "combating poison with poison". That is, the addition of manganese to the water environment may cause secondary contamination. Thus, ensuring an appropriate form of treatment process in which manganese can be completely oxidized by MnOB is the key factor.

Biofiltering is one of the applications of a biofilm that enables enrichment of functional bacteria in the filter bed and intercepts solid suspended materials. Therefore, it can simultaneously achieve the cultivation of MnOB and the accumulation of MnO_x in the filter bed, favoring the degradation process. At present, biofilter is used to remove manganese from drinking water. It was found that the influent manganese at ~2.0 mg/L is effectively removed by the biofilter. MnOB has good adaptability in the co-presence of iron, ammonia, phosphate, and COD (Abu Hasan et al., 2013, 2014; Cai et al., 2018; Tekerlekopoulou et al., 2013). Thus, the biofilter can avoid additional contamination when manganese is used as a feeding agent, which in turn provides a convenient approach to the *in situ*–degradation of antibiotics. It should be noted that filtration is a necessary step for the deep-treatment of wastewater and purification of drinking water. Thus, this approach based on biofiltration is feasible. On the other hand, bioactivity is the key factor in any bio-treatment process, which may be affected by antibiotics, resulting in the change of the bacterial structure. Therefore, the influence of antibiotics on the biofilter or MnOB should be clearly understood.

Therefore, using manganese as a feeding agent, the objectives of this study are to: (1) investigate the degradation of antibiotics mediated by MnOB in a biofilter; (2) study the influence of antibiotics on MnOB; and (3) survey the characteristics of the bacterial community.

1. Materials and methods

1.1. The lab-scale biofilter

The lab-scale biofilter used in this study operates in the up-flow mode as shown by Fig. 1. The biofilter is made of an acrylic glass tube with a diameter of 60 mm. The filter layer with a total height of 30 cm is filled with quartz sand, and the cobblestone support layer at the bottom is 5 cm high. The particle sizes of the quartz sand and cobblestone are 0.6-1.2 mm and 1-3 cm, respectively. Moreover, it is equipped with two peristaltic pumps, an influent tank, a backwash tank, and an air compressor. The spacing between the three water sample ports is 10 cm. The empty bed contact time (EBCT) was calculated using Eq. (1):

$$\mathrm{EBCT} = V/Q \tag{1}$$

where, Q (L/hr) is the water flow, and V (L) is the volume of filter bed.

100 mL of backwash wastewater, which contains MnO_x and bacteria (conc. 0.5 g/L), was collected from a biofilter that was used to remove manganese, and inoculated into the filter bed to achieve the start-up period (Appendix A Fig. S1). The influent was simulated by adding manganese sulfate, ciprofloxacin (CIP), or ceftriaxone (CEF) to tap water. All chemical reagents were purchased from Aladdin Biochemical Technology Co. Ltd. (Shanghai, China). The operational conditions of the biofilter are provided in Appendix A Table S1. The MnO_x gradually accumulates with the operation of the biofilter resulting in pore blocking and formation of a cake layer without backwash. Therefore, backwash was carried out every 3–5 days to maintain the normal operation of the biofilter.

1.2. Kinetic analysis

First-order kinetic reaction mode was successfully applied to describe manganese removal in the biofilter (Cai et al., 2015). Therefore, Eq. (2) was used in this experiment to confirm the influence of CEF and CIP on the removal performance of manganese:

$$\frac{dC_t}{dt} = -kC_t \tag{2}$$

where, k (min^{-1}) is the rate constant; t (min) and C_t (mg/L) are the EBCT and Mn(II) concentration at each sample port. For calculation purposes, the variables in Eq. (2) should be separated and subsequently integrated as shown in Eq. (3):

$$\ln C_t - \ln C_0 = -kt \tag{3}$$

Thus, k will be obtained based on the linear function relation between $\ln(C_t/C_0)$ and t. C_0 (mg/L) is the initial influent manganese concentration.

1.3. Bacterial growth analysis

The influence of antibiotics on MnOB growth was assessed using an automatic microbial growth curve analyzer (Bioscreen C, Oy Growth Curves Ab Ltd., Finland). A modified low-nutrient PC medium was prepared by adding 0.02 g $MnSO_4{\cdot}4H_2O$ to 1 L of tap water (Nealson, 2006). Then, antibiotics (CEF and CIP) were added to the PC medium at the levels of 50, 100, 500, and 1000 ng/L. Considering that the backwash wastewater contains MnO_x and bacteria, after 0.5 hr of precipitation, its suspension was taken as the inoculum. A total of 400 µL of mixture containing 350 µL of PC medium and 50 µL of inoculum was loaded on to the sample plate. The culture temperature was 25°C. The type of shaking, amplitude, and speed were chosen as continuous, medium, and normal, respectively. Under this mode, the duration of shaking is 60 sec, the interval is 10 sec, and the stop is 8 sec before measurement. The measurement interval was set at 24 hr and the growth curve was monitored at 600 nm until it stopped growing. As a comparison, the medium without antibiotics was set as the blank control.

The bacterial growth process is described according to Eq. (4):

$$X = X_0 e^{\mu t} \tag{4}$$

where, t (hr) is the culture time; X_0 (Abs) is the initial optical density (OD_{600}) at $t = 0$; X (Abs) is the OD_{600} value at the culture time t; µ (hr^{-1}) is the specific growth rate. µ can be obtained by converting Eq. (4) to the natural logarithm form as in Eq. (5):

$$\ln \frac{X}{X_0} = \mu t \tag{5}$$

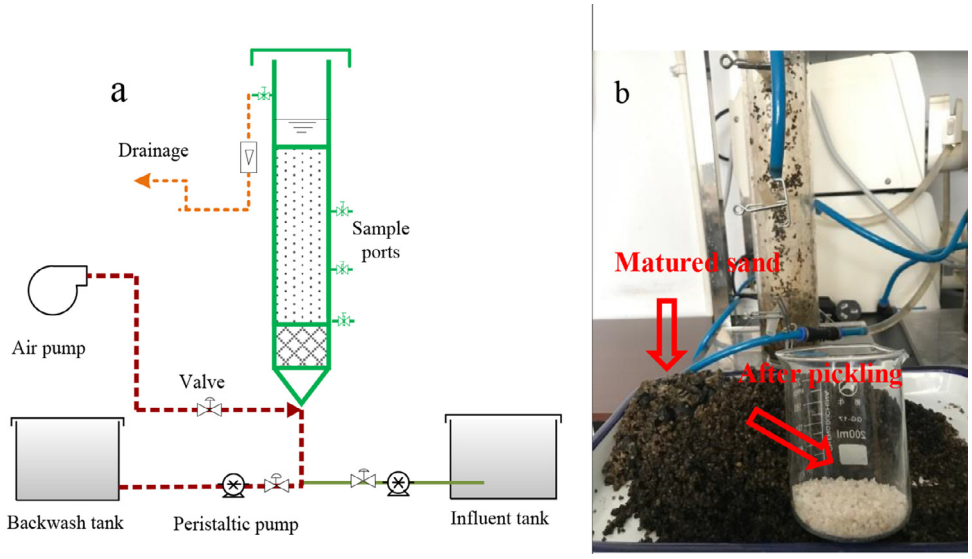

Fig. 1 – The lab-scale biofilter used in this study: (a) schematic diagram of the biofilter; (b) the matured quartz coated by MnO_x and after acid wash.

1.4. *Sample analysis*

The concentration of manganese was measured by a built-in program of potassium periodate spectrophotometry on a multi-parameter water quality analyzer (Lianhua5B-3B, China). CEF and CIP were measured using ultra high-performance liquid chromatography-mass spectrometer (HPLC-MS, Triple Quad™ 3500, AB SCIEX, USA).

The biogenic MnO_x collected from the backwash procedure was characterized by methods of X-ray diffraction (XRD, Ultiman IV, Rigaku, Japan), transmission electron microscopy (TEM, FEI-F20, USA), optical microscopy (IX70, Olympus, Japan), X-ray photoelectron spectroscopy (XPS, Escalab 250Xi, Thermo Scientific, USA), BET surface area (ASAP 2460, Micromeritics, USA), and energy dispersive X-ray spectroscopy (EDS, Oxford, USA). Meanwhile, experiments were conducted to assess the reaction process of the biogenic MnO_x with CEF and CIP.

1.5. *DNA extraction, library construction, and metagenomic sequencing*

15 g of wet sand sample was collected from the biofilter at 25 days and the end of the operation of the biofilter (named MnO_x and CEF). Total genomic DNA was extracted using FastDNA SPIN Kit for Soil (MP Biomedicals, CA, USA) according to the manufacturer's instructions. Concentration and purity of the extracted DNA was determined with TBS-380 and NanoDrop 2000, respectively. DNA extract quality was checked on 1% agarose gel.

DNA extract was fragmented to an average size of about 400 bp using Covaris M220 (Gene Company Ltd., China) for paired-end library construction. Paired-end library was constructed using NEXTflex™ Rapid DNA-Seq Kit (Bioo Scientific, Austin, TX, USA). Adapters containing the full complement of sequencing primer hybridization sites were ligated to the blunt-end of fragments. Paired-end sequencing was performed on a Novaseq platform (Illumina Inc., San Diego, CA, USA) at Majorbio Bio-Pharm Technology Co. Ltd. (Shanghai, China) using NovaSeq Reagent Kits/HiSeq X Reagent Kits according to the manufacturer's instructions (www.illumina.com). There are 47,676,552 and 46,076,932 raw reads after sequencing for MnO_x and CEF, respectively. After sequence quality control, genome assembly, gene prediction, and non-redundant gene catalog construction, representative sequences of a non-redundant gene catalog were aligned to the NCBI NR database with an e-value cutoff of $1e^{-5}$ using BLASTP (Version 2.2.28+, http://blast.ncbi.nlm.nih.gov/Blast.cgi) for taxonomic annotations. Antibiotic resistance annotation was conducted using BLASTP search against CARD database (http://arpcard.Mcmaster.ca, version 1.1.3) with "strict" comparison.

2. Results and discussion

2.1. *The operation of biofilter*

According to the proposed approach, manganese was used as a feeding agent of the biofilter. Then, the simultaneous degradation of antibiotics during the operation of the biofilter was studied. Meanwhile, the effect of hydraulic loading and feeding manganese loading on the degradation process were also assessed.

2.1.1. *The simultaneous removal of manganese and antibiotics*

During the operational stage I, II, and III, the feeding manganese was prepared to the concentrations of 0.3 and 0.6 mg/L at each stage. Antibiotics were added to the influent flow after stage I. Fig. 2 shows the operational results of the biofilter.

At stage I, it could be seen that the feeding manganese could be removed by the biofilter even if it increased from 0.3 to 0.6 mg/L. The effluent manganese was always below the detection limit. As compared to stage I, the feeding manganese at stages II and III could still be effectively removed even with the addition of antibiotics. It indicated that the antibiotics, at least at the 50 ng/L level, could not affect the capacity of the biofilter. Meanwhile, the average CIP removal efficiency at stage II was 11.3% and 21.8%, and at stage III it was 13.3% and 22.7% for CEF (Fig. 2). The antibiotic removal was enhanced with the increase in the feeding manganese. It was observed that the linear coefficients between the antibiotics removal and the feeding manganese were 17.6 ng/mg (CIP)

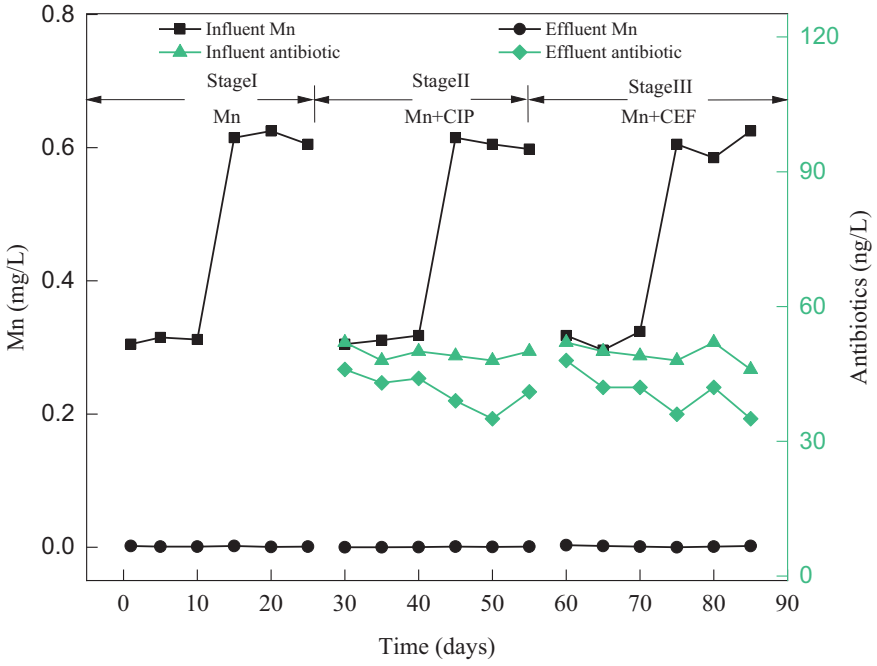

Fig. 2 – The operational results of the biofilter for simultaneous removal of manganese and antibiotics.

and 18.8 ng/mg (CEF) (Appendix A Fig. S2). It should be noted that these coefficients might be slightly higher than the actual values because of some unknown removal contributions, for example, the adsorption by sand although it was coated with MnO_x. Sabirova et al. (2008) demonstrated that the degradation of 17α-ethinylestradiol was not dependent on the presence of bacterial cells, but rather on the amount of biogenic manganese oxides produced. It seems that MnOB plays an indirect role in the degradation process. The high feeding manganese loading indicates high biomass or bioactivity to some extent. Therefore, the removal of antibiotics, which was directly achieved by MnO_x, may be also affected by the biomass concentration.

2.1.2. *Effect of hydraulic and influent manganese loading on antibiotics removal*

The influence of the hydraulic loading and the feeding manganese on antibiotic removal was studied and presented in Fig. 3. In Fig. 3a, the feeding manganese loading was maintained at 28.8 mg/day, and the hydraulic loading was 48, 96, and 144 L/day. It was found that the removal of CIP and CEF had no significant change at these hydraulic loading levels. The average removal efficiency for CIP and CEF was 20.8% and 20.6%, respectively. Antibiotics could be removed as long as manganese was removed. In Fig. 3b, the hydraulic loading was set at 48 L/day, and the loading of the feeding manganese was improved since stage III from 14.4 m/day and 28.8 m/day to 43.2 mg/day. The average removal efficiency for CIP and CEF increased to 33.4% and 33.2%, respectively. This further demonstrated that the removal of antibiotics was the result of MnO_x. Meanwhile, the linear relationship between the removal loading of antibiotics and the feeding manganese was 18.09 ng/mg for CIP ($R^2 = 0.99$) and 18.13 ng/mg for CEF ($R^2 = 0.99$), which was similar to the values obtained in Section 2.1.1. Adsorption is usually followed by degradation. In Sections 2.1.1 and 2.1.2, the removal of CIP and CEF seems to be at a similar level. This may be dominated by physical adsorption, although electrostatic attraction could be another pathway (Cai et al., 2018).

Since the antibiotics are at a very low level, it is difficult to identify the degradation process. It can be seen from Eq. (6) that the catalytic degradation of organic matter by MnO_2 depends on pH. The release of manganese is an indicator for the degradation.

$$MnO_2 + 4H^+ + 2e^- \xrightarrow{\text{catalytic}} Mn^{2+} + 2H_2O \quad (6)$$

In order to confirm that the biogenic MnO_x conforms to Eq. (6), the reaction between the high quantity of antibiotics was constructed. In Fig. 3c, at pH 4 and 7, the release of manganese from the blank control without CIP addition was lower than that in the presence of CIP. This revealed that the degradation process was mediated by the biogenic MnO_x. On the other hand, the release of manganese at pH 4 was higher than that at pH 7 (Fig. 3c), which was similar to the CEF degradation in Fig. 3d. Obviously, the removal of antibiotics by MnO_x conformed to Eq. (6). Moreover, in Fig. 3c and d, the release of manganese increased after the sterilization of the matured sand by ultraviolet indicating the role of MnOB.

2.2. *Effect of antibiotics on the biofilter*

The activity of MnOB is an important factor that affects the generation of MnO_x. The profiles of manganese between the influent and effluent demonstrated that the activity of MnOB could not be affected by CEF and CIP (Fig. 2). However, it was possible that the MnOB activity was severely reduced by antibiotics as this may be compensated as long as the filter layer was high enough.

2.2.1. *Kinetic analysis*

The removal of manganese was kinetically analyzed along the filter bed at the total EBCTs of 0.34 and 0.70 hr. Table 1 presents the kinetic analysis results based on the first-order kinetic model (Cai et al., 2015). Then, the influence of CEF and CIP on the MnOB activity was evaluated by comparing the rate constant k value.

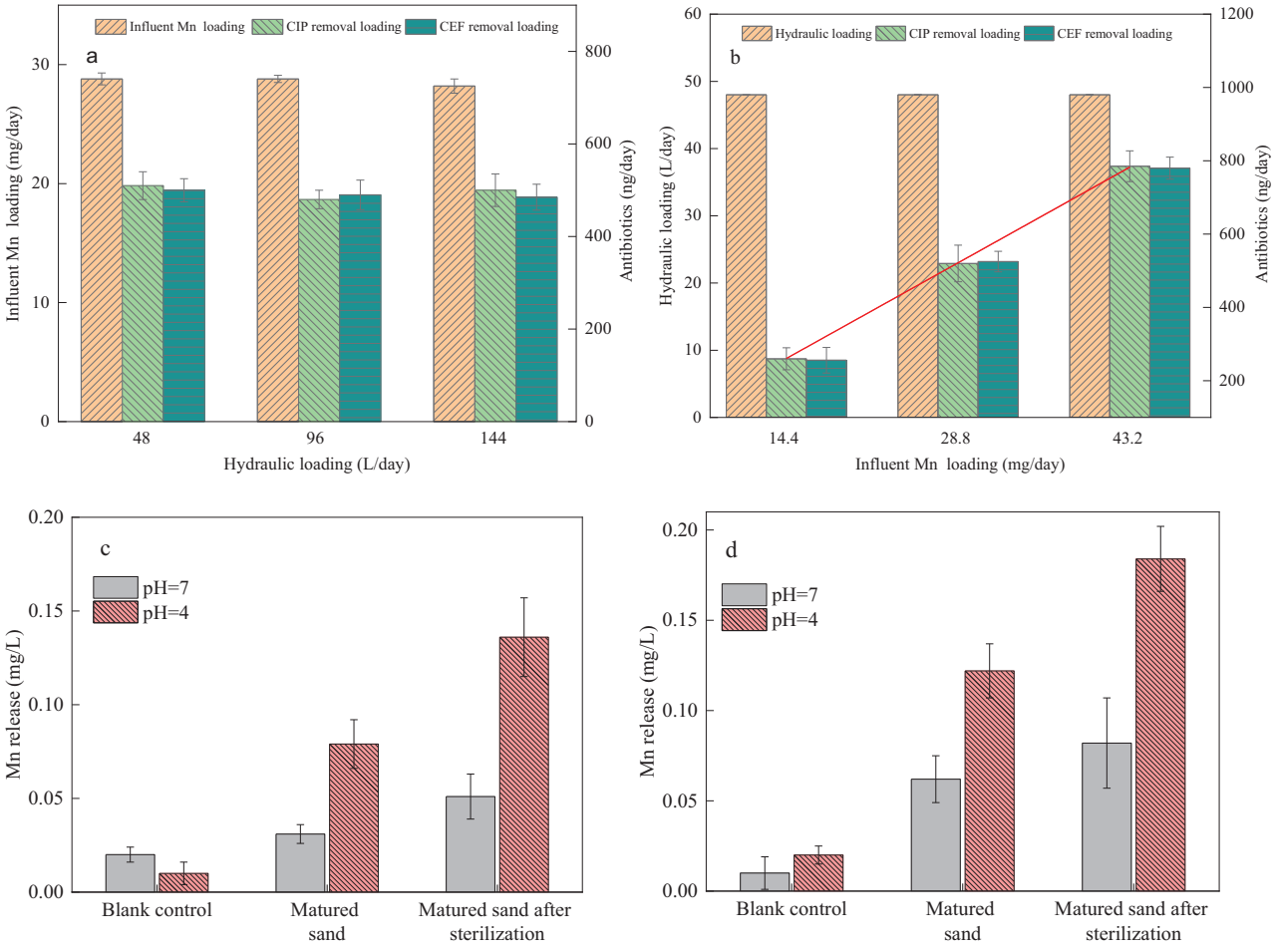

Fig. 3 – The effect of (a) hydraulic loading and (b) influent manganese loading on the antibiotics removal and the release of manganese during (c) CIP degradation (CIP, 5 mg/L, sand=10 g/L) and (d) CEF degradation (CEF, 5 mg/L, sand 10g/L).

Table 1 – Kinetic removal of Mn(II) in the presence of CEF and CIP.

Total EBCT	Influent Mn (mg/L)	Antibiotics	k (min^{-1})	R^2
0.70 hr	0.3	blank	0.144±0.003	0.98
		CEF	0.147±0.005	0.97
		CIP	0.146±0.005	0.99
	0.6	blank	0.145±0.008	0.99
		CEF	0.152±0.007	0.98
		CIP	0.149±0.008	0.99
0.34 hr	0.3	blank	0.264±0.004	0.97
		CEF	0.276±0.009	0.94
		CIP	0.275±0.005	0.96
	0.6	blank	0.262±0.003	0.99
		CEF	0.284±0.004	0.95
		CIP	0.276±0.006	0.98

EBCT: empty bed contact time.

At the total EBCT of 0.70 hr, when the feeding manganese level was 0.3 mg/L, the k with the addition of CEF and CIP was 0.147 min^{-1} and 0.146 min^{-1}, respectively. They were slightly higher than the blank control k value of 0.144 min^{-1}. Meanwhile, the k value increased to 0.152 min^{-1} and 0.149 min^{-1}, as the feeding manganese increased to 0.6 mg/L. It seems that the CEF and CIP enhanced the removal kinetics compared to the blank test. Meanwhile, a similar phenomenon could be observed at a shorter total EBCT of 0.34 hr (Table 1). The k value was also enhanced by a shorter EBCT. This revealed that the loading of the feeding manganese was a limiting factor in removing manganese rather than the antibiotics. The k values at 0.70 hr is slightly lower than 0.174 min^{-1} obtained by Katsoyiannis and Zouboulis (2004), but they increase at 0.34 hr.

2.2.2. *Growth rate of MnOB*

It is well known that antibiotics could inhibit bacterial activity, but Table 1 reveals inconsistent results. Therefore, the growth characteristics of the MnOB group with various levels of antibiotics were further surveyed. It was found that the entire growth process lasted about 10 days, including the growth phase of 1-7 days and the stable phase of 8-10 days (Appendix A Fig. S3). According to Eq. (5), the bacterial growth rate could be obtained by linearly fitting the growth curve at the growth phase (1-7 days) as shown in Table 2.

The statistical results indicated that the growth rates of MnOB at antibiotic levels of 50 and 100 ng/L were higher than that of the blank control test indicating high bioactivity, which is consistent with the kinetics analysis results presented in Table 1. However, the MnOB growth rates were inhibited at other antibiotics levels, and the degree of inhibition increased

Table 2 – The growth rate of MnOB at the antibiotics level of 50 -1000 ng/L.

Antibiotics	Level (ng/L)	μ (hr^{-1})	R^2
None	-	3.81×10^{-4}	0.98
CIP	50	6.20×10^{-4}	0.99
	100	4.07×10^{-4}	0.98
	500	3.55×10^{-4}	0.99
	1000	3.06×10^{-4}	0.97
CEF	50	7.83×10^{-4}	0.97
	100	4.46×10^{-4}	0.96
	500	3.41×10^{-4}	0.99
	1000	2.91×10^{-3}	0.98

CIP: ciprofloxacin; CEF: ceftriaxone.

as the antibiotics increased from 100 to 500 ng/L and 1000 n/L. The antibiotic level of 100 ng/L appeared to be the boundary for the inhibition or promotion of the growth rate of MnOB. Generally, levels of antibiotics that appeared in drinking water resources, rivers, or discharge of wastewater treatment plants were < 100 ng/L (Zhang et al., 2015). Thus, the degradation of antibiotics was mediated by MnOB as an alternative as their activity was at least not inhibited.

Tebo et al. (2004) reported that the enzyme catalytic oxidation of manganese by the MnOB group occurred on an exopolymer matrix surrounding the cell, forming an MnO_x-film on the outer layer of MnOB. The MnO_x was a fibrous-like oxide that twined and twisted together, and its size was about 200 μm (Appendix A Fig. S4). In such an instance, it could block and subsequently degrade a certain amount of antibiotics as demonstrated. As a response to antibiotics, it could be inferred that the MnOB would exhibit a relatively high activity to form the MnO_x-film rapidly, which could protect their activity from being inhibited. However, as the antibiotics exceeded the level that MnOB could tolerate, their activity would be suppressed as shown in Table 2.

2.3. *Characterization of MnO_x by BET surface area, XRD, and XPS*

The biogenic MnO_x has a BET surface area of 39.1 m^2/g, which was lower than the synthetic manganese oxides (Li et al., 2015; Mahamallik et al., 2015) that may be due to the big particle size of MnO_x (~200 μm). Actually, the biogenic MnO_x were constructed by smaller nanoparticles (Su et al., 2014), but they aggregated together and formed nuclei during the accumulation in the filter bed (Appendix A Fig. S4a). That is, the newly formed MnO_x in the nanoscale could contribute to the degradation process suggesting that the degradation of antibiotics could be immediately enhanced as the influent manganese increased (Fig. 2).

The XRD spectrum revealed that the biogenic MnO_x sample contained a characteristic strong peak of SiO_2 at $2\theta = 26.64°$ (PDF#77-1060) that may cause by the friction between the quartz sand during the backwash. Three main characteristic peaks of buserite at $2\theta = 8.75°$, 17.69°, and 26.67° (PDF#32-1128) were also observed from the XRD spectrum (Appendix A Fig. S5). It seems that the biogenic MnO_x appeared to be a precursor of the buserite-like material, which is considered the hydrated form of birnessite. However, the structure of MnO_x could not be further determined due to its amorphous form. Anyhow, the degradation of antibiotics by the MnO_x suggested in this paper is consistent with the fact that the manganese ores could degrade a variety of organic matter (Remucal and Ginder-Vogel, 2014).

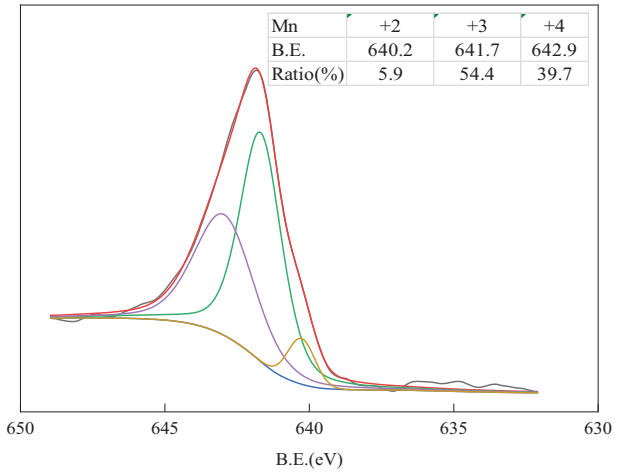

Fig. 4 – Characterization of the biogenic MnO_x by XPS.

Meanwhile, three characteristic peaks at 640.2, 641.7, and 642.9 eV were obtained from the XPS spectrum after peak fitting (Fig. 4), which indicated Mn(II), Mn(III), and Mn(IV), respectively. They contributed 5.9%, 54.4%, and 39.7%, respectively, to the MnO_x, and the average oxidation state was +3.34. However, Su et al. (2014) found that the biogenic manganese oxide was rich in Mn(II) (53.6%). The most probable reason for this was the difference in the bio-system. Tu et al. (2014) also found that the contribution of manganese was significantly dependent on the reaction conditions (e.g., pH) even if for the single bacterium strain. The degradation capacity between the different manganese oxides was different (Liu et al., 2009), but being rich in Mn(III) or Mn(IV) would to some extent favor the electron transfer process during the degradation. Both Mn(III) and Mn(IV) contributed to 94.1% to the MnO_x indicating that using the biofilter for *in situ* generation of manganese oxide was a feasible approach to control the antibiotics contamination.

2.4. *Bacterial community*

Bacteria played an important role in indirectly driving the degradation process, and thus, the influence of antibiotics on their community was investigated.

2.4.1. *Bacterial structure and function*

Bacteria was the key factor in driving the MnO_x-mediated degradation process, but it indicated that the bacterial species in the biofilter had apparently no change in the presence of antibiotics (Appendix A Fig. S6). Fig. 5a further revealed that the two samples (named MnO_x and CEF) contained the same top 25 genera. This suggested that the structure of the bacterial community was stable enough to cope with the effect of antibiotics.

Leptothrix and *Pseudomonas* were two of the well-known MnOB genera, but the former contributed less to the bacterial community in the biofilter (data not shown), and the latter ranked only at 17th. The functional bacteria that were responsible for the oxidation of manganese seemed to be irrelevant to well-reported genera, such as *Crenothrix, Hyphomicrobium*, and *Siderocapsa* (Katsoyiannis and Zouboulis, 2004). Actually, the extracellular polymer that is secreted by the MnOB group was generally associated with multicopper oxidase (Brouwers et al., 2020; Tebo et al., 2004). Because copper appeared in the MnO_x (Appendix A Fig. S7), it thus provides evidence that the biofilter contained some other rarely

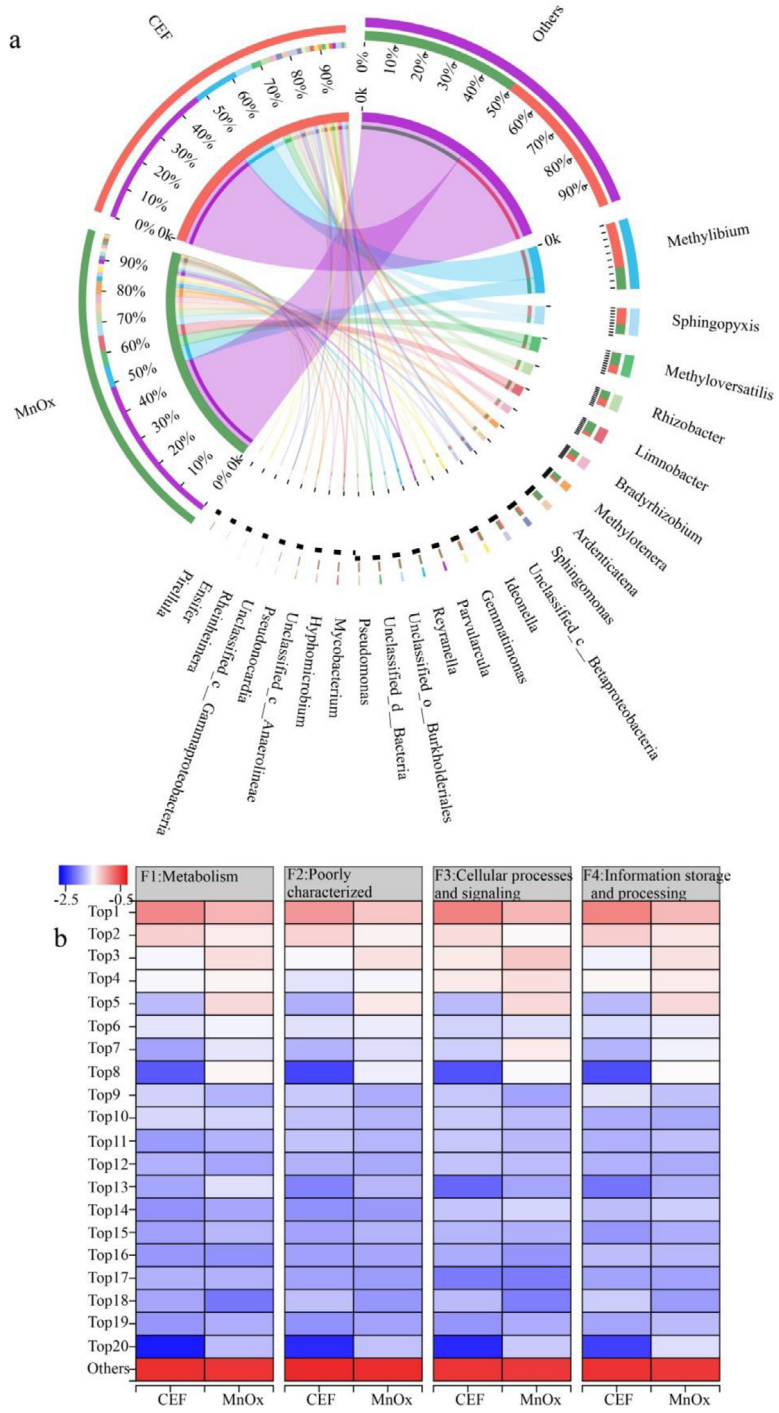

Fig. 5 – (a) The bacterial structure and (b) cellular functions.

reported MnOB group. That is, the well reported genera need not be present in the biofilter (Cai et al., 2015). Some species that were found in Mn deposits or mines could also dominate in the biofilters, such as *Methylibium* reported in this paper (Sjöberg et al., 2018).

Although the bacterial structure did not significantly change as shown in Fig. 5a, the bacterial activity was affected (Tables 1 and 2). The activity of MnOB can be reflected by cellular functions: metabolism, cellular processes and signaling, and information storage and processing. Fig. 5b shows that the functional contribution of *Methylibium* (top1) and *Sphingopyxis* (top2) became significantly higher in the presence of antibiotics. By contrast, the functional contribution of *Methyloversatilis* (top3), *Limnobacter* (top5), *Methylotenera* (top7), *Ardenticatena* (top8), *Parvularcula* (top13) and unclassified *Anaerolineae* (top20) decreased. The other species only had slight change in the presence of antibiotics. Then, it could be known that not all the bacterial activity was promoted by the antibiotics (50 ng/L). The performance of the biofilter or the activity of the MnOB group seemed to rely on the primary dominant genus such as the top1 and top2 presented here.

Table 3 – The abundance of ARGs detected in the biofilter.

AGRs	Antibiotic type	MnO_x	CEF
Sul1	sulfonamide	72	156
Sul2	sulfonamide	34	28
APH(3′′)-Ib	aminoglycoside	2	14
APH(6)-Id	aminoglycoside	2	32
Aminoglycoside related	-	22	18

AGRs: antibiotic resistance gene.

2.4.2. *Antibiotic resistance gene (ARGs)*

The bacteria that are inhibited or induced by antibiotics may express ARGs, it is undesired especially for any bio-system. More than 6.5×10^5 ARGs–related genes were obtained for the two samples (MnO_x and CEF). Table 3 shows that the ARGs that have a shared identity of $\geq$ 98% with those known ARGs having very low abundance. They could be classified into two major groups: sulfonamide-RG (Sul1 and Sul2) and aminoglycoside-RG. However, CEF and CIP belonged to β-lactams and fluoroquinolones, respectively, suggesting that the bacteria in the biofilter were not induced by antibiotics to generate RGs. Because antibiotics are microbial metabolites, most of them possess genes that can encode resistance to the compounds that they produce. These are the quasi-resistance genes that are intrinsically resistant genes of bacteria, and that is the reason for the presence of ARGs in the absence of any antibiotics or exposure (Davies, 2011). As compared to the MnO_x sample, there is no generation of new type of ARGs from the CEF sample. Therefore, at a moderate antibiotics level, this approach could prevent additional generation of ARGs. This further demonstrated the feasibility of this approach.

3. Conclusion

During the oxidation of the feeding manganese using a biofilter, the *in situ* product of MnO_x could be used to control trace antibiotics contamination. The degradation of antibiotics could be ensured as long as the feeding manganese was well removed, showing a linear function. The XRD and XPS analysis further demonstrated the degradation capacity of MnO_x. Although the cellular processes of bacterial genera in the biofilter were promoted or inhibited by antibiotics, the bacterial community was structurally stable and no generation of additional ARGs were evidenced in the biofilter. Importantly, the activity of the MnOB group was promoted at the antibiotic levels of 50 and 100 ng/L. As the antibiotics in drinking water or discharge of wastewater treatment plants are usually below 100 ng/L, this approach is feasible in controlling antibiotic contamination.

Acknowledgment

This work was supported by the National Key R&D Program of China (No. 2017YFC0403404) and the Shandong Provincial Natural Science Foundation (No. ZR2016EEQ30) .

Appendix A Supplementary data

Supplementary material associated with this article can be found, in the online version, at doi:10.1016/j.jes.2020.05.024.

REFERENCES

Abu Hasan, H., Sheikh Abdullah, S.R., Kamarudin, S.K., Kofli, N.T., Anuar, N., 2013. Simultaneous NH_4^+-N and Mn^{2+} removal from drinking water using a biological aerated filter system: Effects of different aeration rates. Sep. Purif. Technol. 118, 547–556.

Abu Hasan, H., Sheikh Abdullah, S.R., Kamarudin, S.K., Kofli, N.T., Anuar, N., 2014. Kinetic evaluation of simultaneous COD, ammonia and manganese removal from drinking water using a biological aerated filter system. Sep. Purif. Technol. 130, 56–64.

Bu, Q., Wang, B., Huang, J., Liu, K., Deng, S., Wang, Y., et al., 2016. Estimating the use of antibiotics for humans across China. Chemosphere 144, 1384–1390.

Brouwers, G.J., Vijgenboom, E., Corstjens, P.L.A.M., De Vrind, J.P.M., De Vrind-De Jong, E.W., 2020. Bacterial Mn^{2+} oxidizing systems and multicopper oxidases: An overview of mechanisms and functions. Geomicrobiol. J. 17, 1–24.

Cai, Y., Li, D., Liang, Y., Luo, Y., Zeng, H., Zhang, J., 2015. Effective start-up biofiltration method for Fe, Mn, and ammonia removal and bacterial community analysis. Bioresour. Technol. 176, 149–155.

Cai, Y., Bi, X., Zhang, J., Dong, Y., Liu, W., 2018. Trace amounts of phosphorus removal based on the in-suit oxidation products of iron or manganese in a biofilter. Environ. Sci. 39, 3222–3229.

Davies, J., 2011. Streptomycetes are special: arcane applications. Microb. Biotechnol. 4, 141–143.

Ferri, M., Ranucci, E., Romagnoli, P., Giaccone, V., 2017. Antimicrobial resistance: a global emerging threat to public health systems. Crit. Rev. Food Sci. Nutr. 57, 2857–2876.

Katsoyiannis, I.A., Zouboulis, A.I., 2004. Biological treatment of Mn(II) and Fe(II) containing groundwater: kinetic considerations and product characterization. Water Res. 38, 1922–1932.

Liu, C., Zhang, L., Li, F., Wang, Y., Gao, Y., Li, X., et al., 2009. Dependence of sulfadiazine oxidative degradation on physicochemical properties of manganese dioxides. Ind. Eng. Chem. Res. 48, 10408–10413.

Li, Y., Wei, D., Du, Y., 2015. Oxidative transformation of levofloxacin by δ-MnO_2: Products, pathways and toxicity assessment[J]. Chemosphere 119, 282–288.

Li, L., Wei, D., Wei, G., Du, Y., 2017. Product identification and the mechanisms involved in the transformation of cefazolin by birnessite (δ-MnO_2). Chem. Eng. J. 320, 116–123.

Mahamallik, P., Saha, S., Pal, A., 2015. Tetracycline degradation in aquatic environment by highly porous MnO_2 nanosheet assembly. Chem. Eng. J. 276, 155–165.

Nealson, K.H., 2006. The manganese-oxidizing bacteria. In: Dworkin, M., Falkow, S., Rosenberg, E., et al. (Eds.). In: Proteobacteria: Alpha and Beta Subclasses, 5. Springer, New York, New York, pp. 222–231.

Pal, A., Mahamallik, P., Saha, S., Majumdar, A., 2017. Degradation of tetracycline antibiotics by advanced oxidation processes: application of MnO_2 nanomaterials. Nat. Resour. Eng. 2, 32–42.

Remucal, C.K., Ginder-Vogel, M., 2014. A critical review of the reactivity of manganese oxides with organic contaminants. Environ. Sci. 16, 1247–1266.

Sabirova, J.S., Cloetens, L.F.F., Vanhaecke, L., Forrez, I., Verstraete, W., Boon, N., 2008. Manganese-oxidizing bacteria mediate the degradation of 17α-ethinylestradiol. Microb. Biotechnol. 1 (6), 507–512.

Su, J., Deng, L., Huang, L., Guo, S., Liu, F., He, J., 2014. Catalytic oxidation of manganese(II) by multicopper oxidase CueO and characterization of the biogenic Mn oxide. Water Res. 56, 304–313.

Sjöberg, S., Callac, N., Allard, B., Smittenberg, R.H., Dupraz, C., 2018. Microbial communities inhabiting a rare earth element enriched birnessite-type manganese deposit in the Ytterby Mine, Sweden. Geomicrobiol. J. 35, 657–674.

Tebo, B.M., Bargar, J.R., Clement, B.G., Dick, G.J., Murray, K.J., Parker, D., et al., 2004. Biogenic manganese oxides: properties and mechanisms of formation. Annu. Rev. Earth Planet. Sci. 32, 287–328.

Tekerlekopoulou, A.G., Pavlou, S., Vayenas, D.V., 2013. Removal of ammonium, iron and manganese from potable water in biofiltration units: a review. J. Chem. Technol. Biotechnol. 88, 751–773.

Tu, J., Yang, Z., Hu, C., Qu, J., 2014. Characterization and reactivity of biogenic manganese oxides for ciprofloxacin oxidation. J. Environ. Sci.-China 26 (5), 1154–1161.

Wang, A., Wang, H., Deng, H., Wang, S., Shi, W., Yi, Z., et al., 2019. Controllable synthesis of mesoporous manganese oxide microsphere efficient for photo-Fenton-like removal of fluoroquinolone antibiotics. Appl. Catal. B-Environ. 248, 298–308.

Wang, A., Chen, Z., Zheng, Z., Xu, H., Wang, H., Hu, K., et al., 2020. Remarkably enhanced sulfate radical-based photo-Fenton-like degradation of levofloxacin using the reduced mesoporous MnO@MnOx microspheres. Chem. Eng. J. 379, 122340.

Zhang, Q.Q., Ying, G.G., Pan, C.G., Liu, Y.S., Zhao, J.L., 2015. Comprehensive evaluation of antibiotics emission and fate in the river basins of China: source analysis, multimedia modeling, and linkage to bacterial resistance. Environ. Sci. Technol. 49 (11), 6772–6782.

Zhang, Z., Ruan, Z., Liu, J., Liu, C., Zhang, F., Linhardt, R.J., et al., 2019. Complete degradation of bisphenol A and nonylphenol by a composite of biogenic manganese oxides and Escherichia coli cells with surface-displayed multicopper oxidase CotA. Chem. Eng. J. 362, 897–908.